Structural refinement and photoluminescence properties of cube-like $(Ca_{1-x}Cu_x)TiO_3$ crystals synthesized by the microwave-hydrothermal method

Larissa H. Oliveira[*], Ana P. de Moura[**], Laécio S. Cavalcante[**], Selma G. Antonio[**], Elson Longo[**], José A. Varela[2]

[*]UFSCar, São Carlos, SP, Brazil
[**]Instituto de Química, UNESP, Araraquara, SP, Brasil

ABSTRACT

In this work, $(Ca_{1-x}Cu_x)TiO_3$ crystals with (x = 0, 0.01 and 0.02), labeled as CTO, CCTO1 and CCTO2, were synthesized by the microwave-hydrothermal method at 140ºC for 32 min. XRD patterns (Fig. 1), Rietveld refinement and FT-Raman spectroscopy indicated that these crystals present orthorhombic structure Pbnm. Micro-Raman and XANES spectra suggested that the substitution of Ca by Cu in A-site promoted a displacement of the [TiO6]−[TiO6] clusters adjacent from its symmetric center, which leads distortions on the $[CaO_{12}]$ clusters neighboring and consequently cause the strains into the CaTiO3 lattice. FE-SEM images showed that these crystals have an irregular shape as cube like probably indicating an Ostwald-ripening and self-assemble as dominant mechanisms to crystals growth . The powders presented an intense PL blue-emission.

Keywords: Optical materials;Chemical synthesis; XANES; Luminescence, microcrystals

1. INTRODUCTION

Titanium-based perovskite oxides symbolized as $ATiO_3$ (A= Pb, Sr, Ba, Zn, Ni, or Fe) presents outstanding potential in electronics[1], gas sensors[2], catalysis[3], memory devices[4], magnetic material[5], and so on. Moreover, the photoluminescent (PL) properties were observed in $(Ba,Ca)TiO_3$[6], $Pb(Zr,Ti)O_3$[7], $SrTiO_3$[8], $MgTiO_3$ [9] systems. These compounds present broad and intense PL emission at room temperature that can provide the comprehension of energetic levels, defects formation, surface states, which are intrinsically related to its optical response. Among these titanates, the $CaTiO_3$ presents a good chemical, physical and thermal stability even in some corrosive environments; and it is also employed as component of microwave technology, field devices and sensors [10]. $CaTiO_3$ is known through its use as the host of rare earth-doped, for its applications in integrated light-emission devices, field emission displays (FED's), and all-solid compact laser devices operating in the blue-green region and positive temperature coefficient (PTC) resistors[11]. In the literature, some others rare-earth ions (Pr^{3+}, Nd^{3+}, Sm^{3+}) have been employed in the A-site (Ca^{2+} ions) substitution into $CaTiO_3$ lattice to improve its optical properties[12-14]. Derén *et al[15]* have synthesized $CaTiO_3:Er^{3+}$ nanocrystals (40 nm) by the sol-gel technique. A strong green up-conversion luminescence was verified after a continuous excitation at 980 nm ($^4I_{9/2} \rightarrow {}^4I_{11/2}$). The obtained results show that this material is a good infrared converter.

However, in this work we report for the first time the obtention of calcium copper titanate cube-like $(Ca_{1-x}Cu_x)TiO_3$ crystals with (x = 0, 0.01 and 0.02) by MH method at 140ºC for 32 min. These compounds were structurally and morphologically characterized by X-ray diffraction (XRD), X-ray absorption near-edge structure spectroscopy (XANES), Micro-Raman (MR) spectroscopy, field emission scanning electron microscopy (FEG-SEM). Finally, their optical properties were investigated by ultraviolet-visible (UV-vis) absorption and photoluminescence (PL) measurements.

2.EXPERIMENTAL SECTION

2.1. Synthesis of $(Ca_{1-x}Cu_x)TiO_3$ crystals

$(Ca_{1-x}Cu_x)TiO_3$ microcrystals with different molar ratio (x = 0, 0.01 and 0.02) labeled as CTO, CCTO1 and CCTO2, respectively, were synthesized by the MH method. $CaCO_3$ was dissolved in 25 mL of deionized water giving rise to a transparent solution, following by addition of 0.01 mol of the $[Ti(OC_3H_7)_4]$ under constant stirring. In a similar way, stoichiometric quantities (1.0 and 2.0% molar) of $Cu(NO_3)_2.2.5\ H_2O$ were dissolved into 25 mL of deionized water and was also added to the system. The resulting solution was mixed with 50 mL of a 6 molar of KOH solution. In order to prevent the formation of calcium carbonate as a second phase, nitrogen gas was constantly bubbled to the system. In the sequence, this mixture was transferred to a Teflon autoclave, which was finally sealed and placed in the MH system using 2.45 GHz microwave radiation with maximum power of 800W. The MH conditions were kept at 140ºC for 32 min, using a heating rate fixed at 10ºC/min. Finalized the MH processing, the autoclave was naturally cooled to room temperature. Thus, the solid product was water washed for several times until neutral pH, and then, dried at 75ºC for 12 h.

2.2 Characterizations

The CTO, CCTO1 and CCTO2 microcrystals were structurally characterized by X-ray diffraction (XRD) in normal routine using a Rigaku-DMax/2500PC (Japan) with Cu-Kα radiation (λ = 1.5406 Å) and in the 2θ range from 25 to 64º and 10º to 130º with a scanning rate of 0.02º/min. The MR spectra were obtained using a 488 nm line of a Nd:YAG laser, keeping its maximum output power at 25 mW. Ti and Ca *K*-edge XANES spectra were collected in samples deposited on polymeric membranes, in transmission mode at room temperature with a Si(111) channel-cut monochromator. The spectra were measured from 30 eV below to 150 eV above the edge, with an energy step of 0.3 eV near the edge region. The analysis of the XANES spectra were performed using IFEFFIT package[16]. The crystals morphologies were verified using a Scanning Electron Microscope (Jeol JSM-6460LV microscope). UV-vis absorption spectra of the $(Ca_{1-x}Cu_x)TiO_3$ crystals were performed using a Cary 5G equipment.PL was measured with a 139 Thermal Jarrel-Ash Monospec 27 monochromator and a Hamamatsu R446 photomultiplier. The 350 nm exciting wavelength of a krypton ion laser (Coherent Innova) was used, keeping a nominal output power of 200 mW. All the measurements were performed at room temperature.

3. RESULTS AND DISCUSSION

3.1. X-ray diffraction (XRD)measurements

Fig. 1 shows the XRD patterns of CTO, CCTO 1 and CCTO2 crystals synthesized at 140ºC for 32 min. The results for $(Ca_{1-x}Cu_x)TiO_3$ crystals indicated that these crystals crystallized in a orthorhombic structure with space group *Pbnm*, point group symmetry D_{2h}^{16} and four clusters per unit cell (Z = 4). Moreover, no presence of secondary phases was observed, indicating that the Cu atoms were incorporated in the lattice.

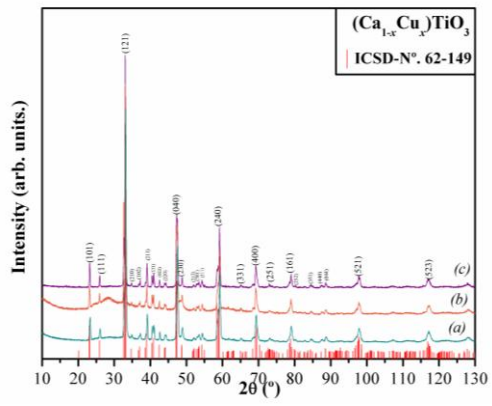

Figure 1: XRD patterns of CTO(a) CCTO1(b) and CCTO2(c) powders processed by microwave-hydrothermal at 140 ◦C for 32min. The vertical dashed lines indicate the position and relative intensity of ICSD card no. 62-149.

3.2. micro-Raman spectroscopy analysis

According to the literature [17,18], the $CaTiO_3$ with perovskite-type orthorhombic structure and space group (*Pbnm*) with four clusters per primitive cell exhibit 24 Raman-active modes. Small changes in polarizability into orthorhombic $CaTiO_3$ lattice, caused by the MH method, can improve the interaction between the ions and also promote the overlapping of some Raman active modes with modes of minor intensity. Thus, only nine Raman active modes (P_1, P_2, P_3, P_4, P_5, P_6, P_7, P_8 and P_9) were detected in the MR spectra of $(Ca_{1-x}Cu_x)TiO_3$ crystals. The MR spectra of these crystals are presented at Fig. 2(a-c).

As the concentration of Cu^{2+} increases up to x = 0.02 in the $CaTiO_3$ lattice (Figs. 4 a-c) slight shifts were observed on the characteristic positions of Raman peaks, comparing to the pure $CaTiO_3$. These changes can be related to the symmetry breaking of the $[CaO_{12}]$ clusters caused by the introduction of copper in the A-site into the $CaTiO_3$ matrix The Raman active modes situated at 714, 693 and 723 cm^{-1} (P_9) for the CTO (Fig. 2(a)), CCTO1 (Fig. 2(b) and CCTO2 (Fig. 2(c)) crystals, respectively, present a more evident shift with increase of Cu content into $CaTiO_3$ lattice.

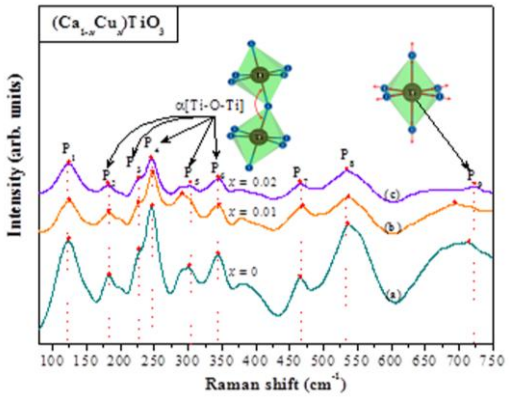

Figure 2: Raman spectra of (a) CTO, (b) CCTO1, and (c) CCTO2 crystals.

3.3. XANES spectroscopy analyses

Fig. 3presents the expanded view of Ti *K*-edge XANES(a) and Ca K-edge XANES(b) spectra of CTO, CCTO1 and CCTO2 crystals prepared by MH method, respectively. In these spectra, it was observed a small peak situated at around 4970.8 eV (•), which is attributed to a transition of the 1*s* electron to an unfilled *d* level. Concerning the main pre-edge peak (•) of the $(Ca_{1-x}Cu_x)TiO_3$ crystals(Fig.3(a)), is possible to verified that the pre-edge peak of the $(Ca_{1-x}Cu_x)TiO_3$ crystals presents a increase in the intensity value as the concentration of copper increases from x = 0 to 0.02. In Fig. 3(b) is

illustrated the pre-edge region (•) situated at around 4.040 eV and the XANES spectra of the $CaTiO_3$ and $(Ca_{1-x}Cu_x)TiO_3$ crystals presents a similar profile as reported by ref. [17,18].

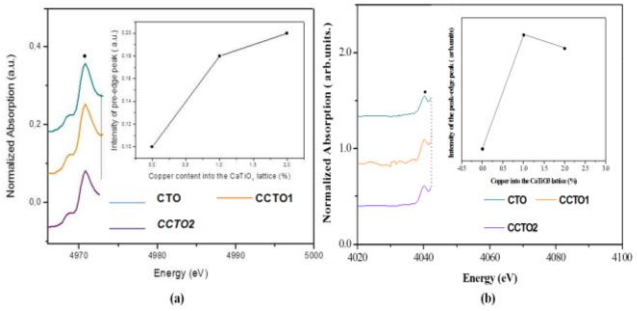

Figure 3. (a) Expanded view of the pre-edge region of normalized Ti K-edge XANES spectra and (b) Expanded view of the pre-edge region of normalized Ca K-edge XANES spectra for the CTO, CCTO 1 and CCTO2 crystals.

As it can be seen in the inset of Fig. 4 (b), the intensity of the pre-edge region (•) for the CTO, CCTO 1 and CCTO 2 also varies with the amount of copper added to these systems.

3.3. UV-vis absorption spectroscopy analyses

Table 2 presents the E_{gap} values of CTO, CCTO1 and CCTO2 crystals synthesized at 140ºC for 32 min in MH system.

The optical band gap energy (E_{gap}) was estimated by the method reported by Wood and Tauc [19]. These authors have explained that the optical band gap is associated with absorbance and photon energy by the following equation (1):

$$h\upsilon\alpha \propto (h\upsilon - E_g)^2, \quad (1)$$

where α is the absorbance, *h* is the Planck constant, *v* is the frequency, E_{gap} is the optical band gap and *n* is a constant associated to the different types of electronic transitions (*n* = 0.5, 2, 1.5 or 3) for direct allowed, indirect allowed, direct forbidden and indirect forbidden transitions, respectively.

For $CaTiO_3$ crystals, the electronic transitions occurs inside the $[TiO_6]$ octahedral clusters, since the 2*p* orbitals of oxygen atoms in valence band and the 3*d* orbitals of the titanium atoms can also be associated to the conduction band (3,2 eV). However, for the $(Ca_{1-x}Cu_x)TiO_3$ crystals, the *3d* orbitals of the copper atoms will be associated to the conduction band[21], so a decrease of the optical gap is observed for 3.0 eV. Moreover, structural defects such as distortions and/or strains in the $CaTiO_3$ lattice leaded to an appearance of intermediary levels between the valence and conduction bands, and an increase in the E_{gap} value is observed for the CCTO2 crystals (3.1 eV).

3.4. Photoluminescence analyses: emission spectra studies

The PL emission spectra of the CTO, CCTO1 and CCTO2 are presented in Fig. 5.

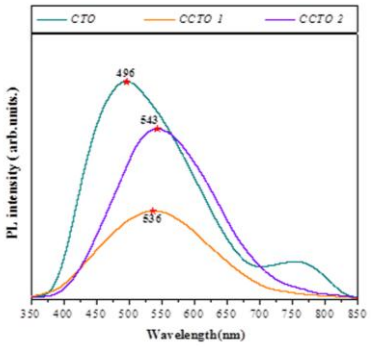

Figure 5. PL spectra of CTO, CCTO1 and CCTO2 crystals processed at 140ºC for 32 min.

As it can be observed in Fig. 5, the pure $CaTiO_3$ crystals have a high PL emission at room temperature with maximum PL emission at 496 nm. As the substitution of Ca by Cu increases in the $(Ca_{1-x}Cu_x)TiO_3$ crystals (CTO and CCTO1), it is noticed a reduction in the intensity of PL emission. Finally the PL emission for CCTO 2 crystals exhibits an increase in the intensity PL emission and also a shift in the maximum intensity of the PL emission to 543 nm. Based on the XANES obtained results, we believe that the symmetry breaking of the $[CaO_{12}]$ and $[TiO_6]$ clusters is responsible for this behavior.

3.5. FE-SEM analyses

Fig. 6 illustrates the FE-SEM images of the: (a) CTO, (b) CCTO1, and (c) CCTO2 crystals, respectively. From these micrographies, it was verified that the crystals are agglomerate and polydispersed. The microwave radiation and the excess of the hydroxyls in the reactional media is able to accelerate the solid particles to elevated velocities, leading to an increase of the interparticle collisions, inducing the effective fusion of these particles at the point of collision. These mechanisms are responsible for the fast nucleation of the $(Ca_{1-x}Cu_x)TiO_3$ small particles, as well as the aggregation of several small particles. This growth mechanism is known as Ostwald ripening mechanism. As the concentration of Cu^{2+} increases up to 0.02, the presence of copper ions in the reactional media promotes the increase of the electrostatic interaction between the ions and the amorphous plates are dissolved and, after that, are condensed in the (100) and (010) directions and the micro-

cubes beginning to grow in these directions (Figs. 6 (b) and (c)).

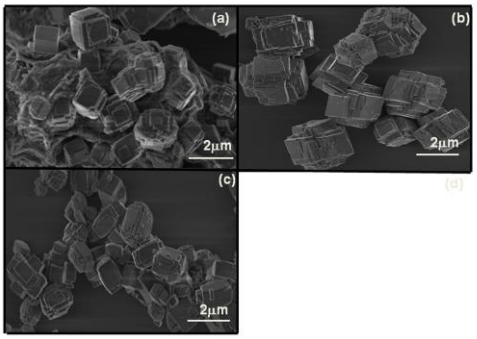

Figure 6. FEG-SEM images of the: (a) CTO, (b) CCTO1, and (c) CCTO2 crystals.

4. CONCLUSIONS

In summary, $(Ca_{1-x}Cu_x)TiO_3$ microcubes were obtained after MH processing at 140°C for 32 min. XRD patterns indicated that these microcrystals crystallize in a $CaTiO_3$ orthorhombic structure with space group (*Pbnm*) without the presence of secondary phases. XANES analysis showed a good agreement with micro-Raman analysis. UV-vis spectra showed a tendency for a reduction in E_{gap} values of crystalline CTO, CCTO 1 and CCTO2 microcrystals, which can be associated to introduction of *3d* orbitals of Copper. The $CaTiO_3$ powder presented an intense PL blue-emission. As the concentration of copper increases it was observed a reduction in the intensity PL emission as well as a shift for green emission up to $x = 0.01$. FE-SEM micrograph showed that the $(Ca_{1-x}Cu_x)TiO_3$ powders are composed by aggregated and polydispersed micro-cubes. Moreover, these micrographs suggested that an Ostwald-ripening mechanism can involved in the formation of these micro-crystals during the MH processing.

5. ACKNOWLEDGEMENTS

The authors are grateful for the financial support of Brazilian agencies CAPES, CNPq and FAPESP.

REFERENCES

[1] W.K. Chen, C.M. Cheng, J.Y. Huang, W.F. Hsieh ,T.Y. Tseng, J. Phys. Chem. Solids 61[6] (2000) 969-977.

[2] R. Parra, R. Savu, L.A. Ramajo, M.A. Ponce, J.A. Varela, M.S. Castro, P.R. Bueno ,E. Joanni, J. Solid State Chem. 183[6] (2010) 1209-1214.

[3] N. Pal, M. Paul ,A. Bhaumik, Appl. Catal. A-General 393[1-2] (2011) 153-160.

[4] M.A. Ramirez, P.R. Bueno, J.A. Varela ,E. Longo, Appl. Phys. Lett. 89 [21] (2006).

[5] T. Yamamoto, Y. Kawashima, Y. Kusakabe, S. Matsuda, Y. Mizuoka, Y. Nakade ,T. Okajima, Journal of Physics-Condensed Matter 21 (10) (2009).

[6] F.V. Motta, A.P.A. Marques, J.W.M. Espinosa, P.S. Pizani, E. Longo ,J.A. Varela, Curr. Appl. Phys. 10[1] (2010) 16-20.

[7] M. Anicete-Santos, M.S. Silva, E. Orhan, M.S. Goes, M.A. Zaghete, C.O. Paiva-Santos, P.S. Pizani, M. Cilense, J.A. Varela ,E. Longo, Journal of Luminescence 127 (2) (2007) 689-695.

[8] E. Orhan, F.M. Pontes, C.D. Pinheiro, T.M. Boschi, E.R. Leite, P.S. Pizani, A. Beltran, J. Andres, J.A. Varela ,E. Longo, J. Solid State Chem. 177[11] (2004) 3879-3885.

[9] E.A.V. Ferri, J.C. Sczancoski, L.S. Cavalcante, E.C. Paris, J.W.M. Espinosa, A.T. de Figueiredo, P.S. Pizani, V.R. Mastelaro, J.A. Varela ,E. Longo, Mat. Chem. Phys. 117[1] (2009) 192-198.

[10] A. Boudali, A. Abada, M.D. Khodja, B. Amrani, K. Amara, F.D. Khodja ,A. Elias, Physica B 405[18] (2010) 3879-3884.

[11] B. Yan ,K. Zhou, J. All. Compd. 398[1-2] (2005) 165-169.

[12] Z.Q. Jiang, Y.H. Wang ,Y. Gong, Chin. Phys. B 19[2] (2010) 027801.

[13] P. Boutinaud, E. Tomasella, A. Ennajdaoui ,R. Mahiou, Thin Solid Films 515[4] (2006) 2316-2321.

[14] A.T. de Figueiredo, V.M. Longo, S. de Lazaro, V.R. Mastelaro, F.S. De Vicente, A.C. Hernandes, M.S. Li, J.A. Varela ,E. Longo, J. Luminescence 126[2] (2007) 403-407.

[15] P.J. Deren, R. Mahiou, R. Pazik, K. Lemanski, W. Strek ,P. Boutinaud, J. Luminescence 128[5-6] (2008) 797-799.

[16] B. Ravel ,M. Newville, Phys. Script. T115 (2005) 1007-1010.

[17] S. de Lazaro, J. Milanez, A.T. de Figueiredo, V.M. Longo, V.R. Mastelaro, F.S. De Vicente, A.C. Hernandes, J.A. Varela ,E. Longo, Appl. Phys. Lett. 90[11] (2007) 111904.

[18] J. Milanez, A.T. de Figueiredo, S. de Lazaro, V.M. Longo, R. Erlo, V.R. Mastelaro, R.W.A. Franco, E. Longo ,J.A. Varela, J.Appl.Phys. 106[4] (2009) 043526.

[19] D.L. Wood ,J. Tauc, Phys. Rev. B 5[8] (1972) 3144-&.

[20] M. Matos ,L. Walmsley, J. Phys. Conds. Matt. 18[5] (2006) 1793-1803.